

# GLOBAL FAST TERMINAL SLIDING MODE CONTROL FOR AN ACTIVE POWER FILTER BASED ON A BACKSTEPPING DESIGN

LIHUA DENG<sup>1,2,3</sup>, JUNTAO FEI<sup>1,2,3</sup>, CHANGCHUN CAI<sup>1,3</sup>

**Key words:** Active power filter (APF), Backstepping, Global fast terminal sliding mode (GFTSM), Sliding mode control, Total harmonic distortion (THD).

This paper presents a new control method for an active power filter that is a combination of backstepping control and global fast terminal sliding mode control. The model order of the power system can be reduced by the backstepping method. The GFTSM control ensures that the tracking error of the system state reaches zero in a finite time. The integral design of the backstepping and GFTSM control can guarantee the control's stability, robustness and speed. Experiments were designed to compare GFTSM backstepping control with single backstepping control using MATLAB/ SIMULINK(R). The validity of the proposed controller for a three-phase three-wire system was demonstrated by the results regarding the total harmonic distortion in the system.

## 1. INTRODUCTION

An APF is widely used to eliminate the current harmonics. The control algorithm of the APF is a key element affecting the filter performance [1].

Backstepping control establishes the control law from the final mathematical model back to the input. The system is divided into several low-level subsystems step by step, and the stability of the subsystem is assured by the Lyapunov framework in each step. Therefore, the backstepping method is suitable for a power system [2, 3]. The sliding mode control is a type of nonlinear control that can be applied in a power filter [4, 5], but a general sliding mode control cannot reach the equilibrium point in a finite amount of time. Thus, a faster sliding mode control [6, 7] should be used.

This paper develops a global fast terminal sliding mode control based on the backstepping design for an APF; this control can achieve a better filtering effect than a single control.

## 2. APF MATHEMATICAL MODELLING

The structure of the main circuit is shown in Fig. 1, which is divided into sources, nonlinear loads and APF.

APF consists of harmonic current detection, current tracking control and compensation current generation. The instantaneous reactive power theory is widely used in harmonic current detection. GFTSM control based on backstepping design is applied to current tracking. Compensation current is produced by means of pulse width modulation (PWM) control.

The operating principle of the APF covers four steps: first, voltage and current are detected. Second, compensation current  $i_k$  ( $k=1, 2, 3$ ) for the three phase case) should be obtained at the same amplitude, but in the opposite phase to the harmonic current. Third, an appropriate current tracking control algorithm is used to gain the Insulated-Gate Bipolar Transistors (IGBT) gate signal, making the IGBT output equal to  $i_k$ . Finally, the compensation current, which can counteract the load harmonic current is fed into the system.

According to circuit theory and the Kirchoff theorem, the following equations can be obtained:

$$\begin{cases} u_1 = L_c \frac{di_1}{dt} + R_c i_1 + u_{1M} + u_{MN} \\ u_2 = L_c \frac{di_2}{dt} + R_c i_2 + u_{2M} + u_{MN} \\ u_3 = L_c \frac{di_3}{dt} + R_c i_3 + u_{3M} + u_{MN} \end{cases}, \quad (1)$$

where  $u_1, u_2, u_3$  are the three phase voltages of the filter access point,  $i_1, i_2, i_3$  are the three phase currents of the filter access point,  $u_{1M}, u_{2M}, u_{3M}, u_{MN}$  are the voltages from the a, b, c, N points to the M point,  $R_c$  is the filter compensation resistance, and  $L_c$  is the filter compensation inductance.

If the three-phase voltages and the currents of the system are approximately balanced, then the following equation is obtained:

$$u_{MN} = -\frac{1}{3} \sum_{m=1}^3 J_m u_{dc} \quad (m=1,2,3), \quad (2)$$

$$J_k = \begin{cases} 1 & \text{when } s_k i_{son} \text{ and } s_{k+3} i_{soff} \\ 0 & \text{when } s_k i_{soff} \text{ and } s_{k+3} i_{son} \end{cases} \quad (k=1,2,3) \quad (3)$$

where  $J_k$  is defined as a switch variable, which denotes the IGBT's work state.  $k=1, 2, 3$  are corresponding to the three phases.  $s_k$  is the insulated-gate bipolar transistor (IGBT).

$u_{dc}$  is the capacitor voltage of the dc-link.

Therefore, (1) is further modified to (4).

$$\begin{cases} \frac{di_1}{dt} = -\frac{R_c}{L_c} i_1 + \frac{u_1}{L_c} - \frac{u_{dc}}{L_c} (J_1 - \frac{1}{3} \sum_{m=1}^3 J_m) \\ \frac{di_2}{dt} = -\frac{R_c}{L_c} i_2 + \frac{u_2}{L_c} - \frac{u_{dc}}{L_c} (J_2 - \frac{1}{3} \sum_{m=1}^3 J_m) \\ \frac{di_3}{dt} = -\frac{R_c}{L_c} i_3 + \frac{u_3}{L_c} - \frac{u_{dc}}{L_c} (J_3 - \frac{1}{3} \sum_{m=1}^3 J_m) \end{cases}. \quad (4)$$

A function of the switching state is defined as  $d_k$ .

$$d_k = J_k - \frac{1}{3} \sum_{m=1}^3 J_m \quad k=1,2,3, \quad (5)$$

where  $d_k$  are nonlinear variables, depending on the IGBT

<sup>1</sup> Hohai University, College of IOT Engineering, Changzhou 213022, China, Email: denglh@hhuc.edu.cn

<sup>2</sup> Hohai University, College of Energy and Electrical Engineering, Nanjing 210098, China

<sup>3</sup> Jiangsu Key Lab. of Power Transmission and Distribution Equipment Technology, Changzhou 213022, China

on/off state of the  $k$  phase.

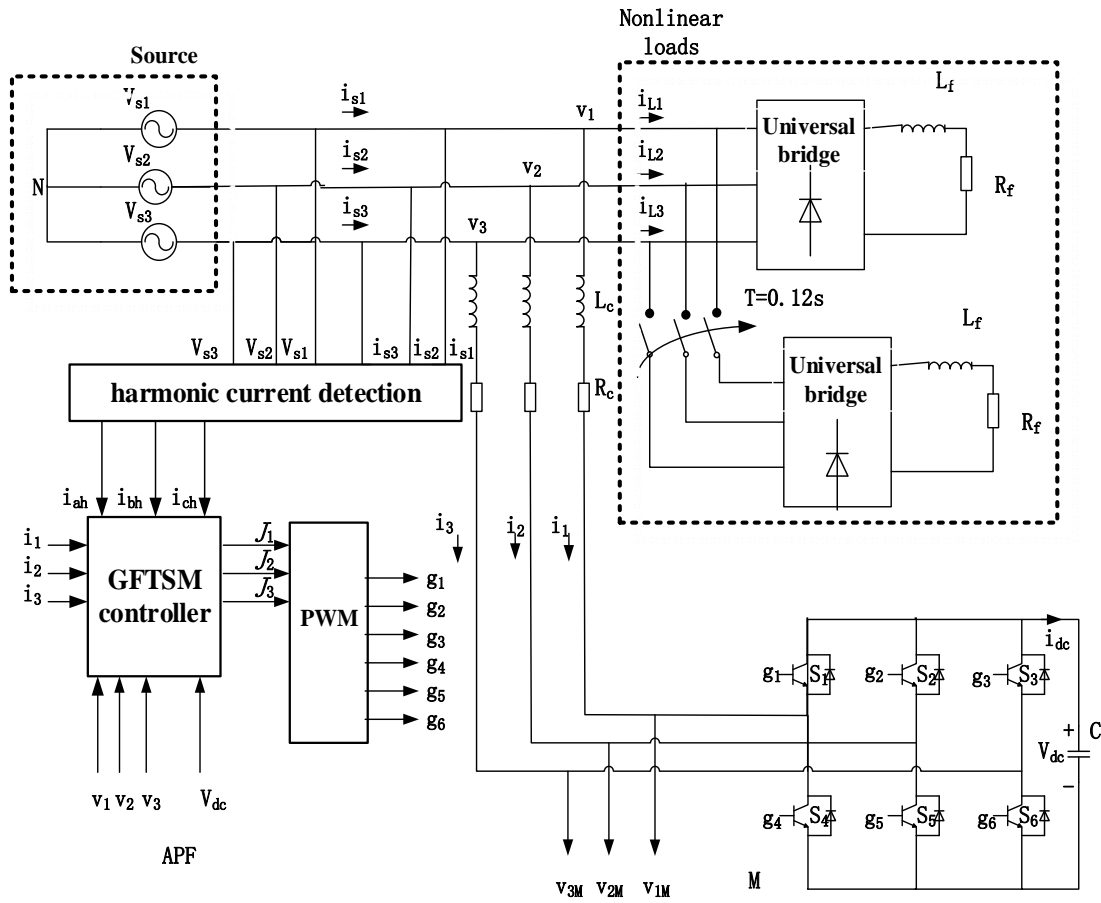


Fig. 1 -Structure of the main circuit.

$$\begin{bmatrix} d_1 \\ d_2 \\ d_3 \end{bmatrix} = \frac{1}{3} \begin{bmatrix} 2 & -1 & -1 \\ -1 & 2 & -1 \\ -1 & -1 & 2 \end{bmatrix} \begin{bmatrix} J_1 \\ J_2 \\ J_3 \end{bmatrix}. \quad (6)$$

Then, (4) becomes (7)

$$\begin{cases} \frac{di_1}{dt} = -\frac{R_c}{L_c} i_1 + \frac{u_1}{L_c} - \frac{u_{dc}}{L_c} d_1 \\ \frac{di_2}{dt} = -\frac{R_c}{L_c} i_2 + \frac{u_2}{L_c} - \frac{u_{dc}}{L_c} d_2 \\ \frac{di_3}{dt} = -\frac{R_c}{L_c} i_3 + \frac{u_3}{L_c} - \frac{u_{dc}}{L_c} d_3 \end{cases}. \quad (7)$$

New state variables are expressed as (8).

$$\begin{cases} x_1 = i_k \\ x_2 = \dot{x}_1 = \dot{i}_k \end{cases} \quad k=1, 2, 3. \quad (8)$$

$$\text{Then, } \dot{x}_1 = \dot{i}_k = -\frac{R_c}{L_c} i_k + \frac{u_k}{L_c} - \frac{u_{dc}}{L_c} d_k$$

$$\begin{aligned} \dot{x}_2 = \ddot{x}_1 = \ddot{i}_k &= -\frac{R_c}{L_c} \dot{i}_k + \frac{1}{L_c} \frac{du_k}{dt} - \frac{1}{L_c} \frac{du_{dc}}{dt} d_k + f(x_1) \\ &= \frac{R_c^2}{L_c^2} x_1 - \frac{R_c}{L_c^2} u_k + \frac{1}{L_c} \frac{du_k}{dt} \\ &= -\frac{R_c}{L_c} \left( -\frac{R_c}{L_c} i_k + \frac{u_k}{L_c} - \frac{u_{dc}}{L_c} d_k \right) + \frac{1}{L_c} \frac{du_k}{dt} - \frac{1}{L_c} \frac{du_{dc}}{dt} d_k \\ &= \frac{R_c^2}{L_c^2} i_k - \frac{R_c}{L_c^2} u_k + \frac{1}{L_c} \frac{du_k}{dt} + \left( \frac{R_c}{L_c^2} u_{dc} - \frac{1}{L_c} \frac{du_{dc}}{dt} \right) d_k \end{aligned} \quad (9)$$

The system state equations are as follows:

$$\begin{cases} \dot{x}_1 = x_2 \\ \dot{x}_2 = f(x_1) + bu, \end{cases} \quad (10)$$

$$\text{where } f(x_1) = \frac{R_c^2}{L_c^2} i_k - \frac{R_c}{L_c^2} u_k + \frac{1}{L_c} \frac{du_k}{dt},$$

$$b = \frac{R_c}{L_c^2} u_{dc} - \frac{1}{L_c} \frac{du_{dc}}{dt}, \quad u = d_k. \quad (11)$$

$x_1$  and  $x_2$  are state variables of the system.  $u$  is the output of the GFTSM controller; in addition,  $u$  is also the input of the system state equations.

### 3. DESIGN

#### OF THE GFTSM BACKSTEPPING CONTROLLER

The design process for the backstepping controller is divided into two steps: first, a virtual control function is constructed. Second, the actual control law is constructed. A controller of phase A is taken as an example.

Step 1. The reference current signal of phase A is the harmonic current,  $i_{ah}$ . The tracking error is defined as  $e_1$ .

If  $e_1 = i_1 - i_{ah} = x_1 - i_{ah}$ , then

$$\dot{e}_1 = \dot{x}_1 - \dot{i}_{ah} = x_2 - \dot{i}_{ah} \quad (12)$$

A new error variable  $e_2$  is defined as a virtual control function.

$$e_2 = x_2 + c_1 e_1 - \dot{i}_{ah}, \quad (13)$$

where  $c_1$  is a positive real number.

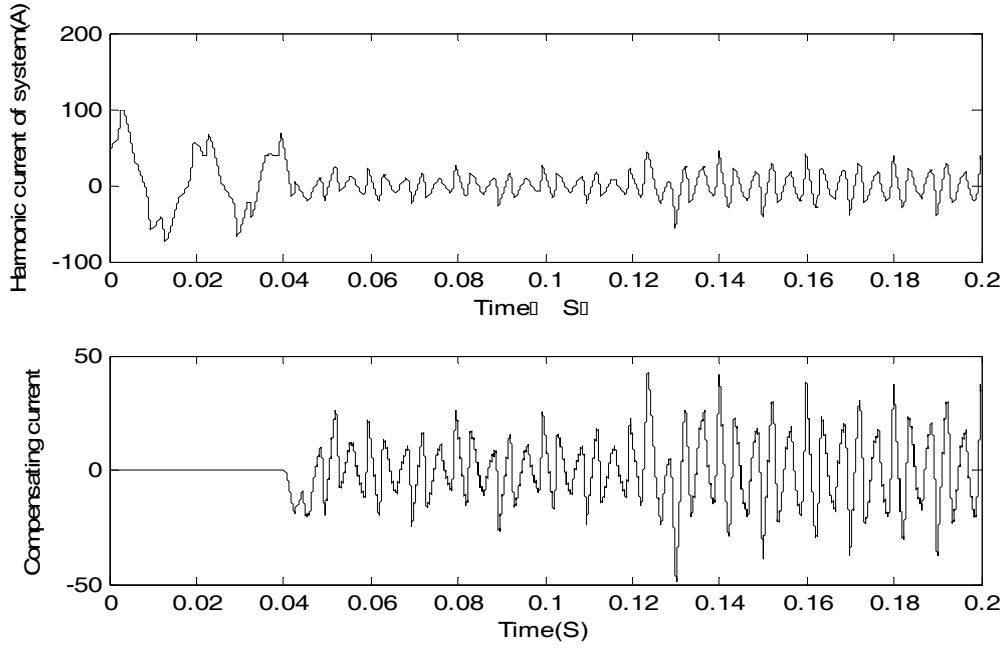


Fig. 2 – Current waveform of load in phase A using the APF.

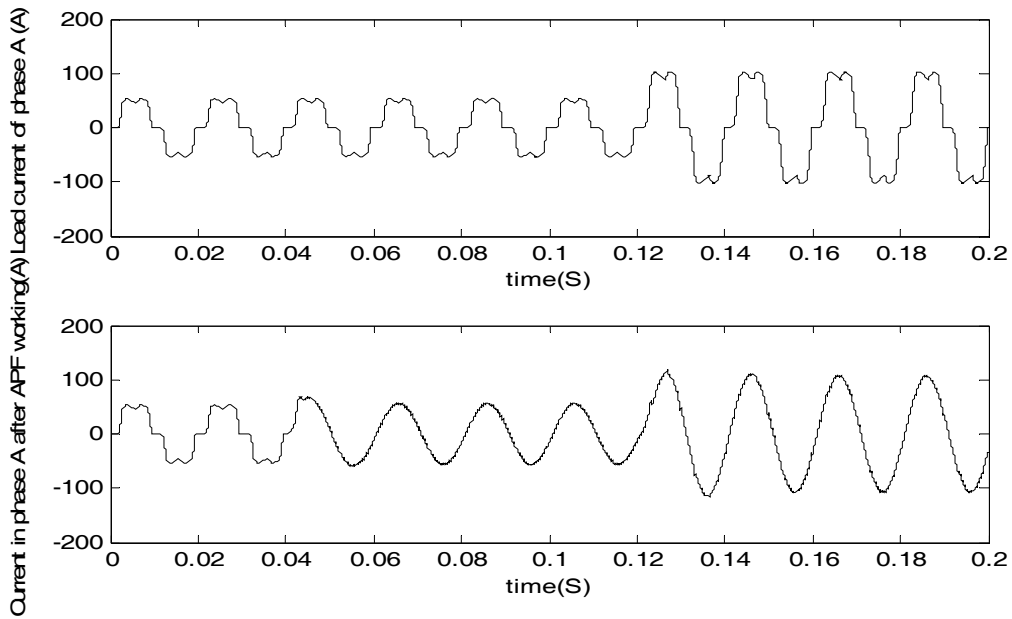


Fig. 3 – The comparison between the harmonic current and the compensating current

A Lyapunov function candidate is defined as follows:

$$V_1 = \frac{1}{2} e_1^2 \geq 0. \quad (14)$$

The derivative of  $V_1$  becomes

$$\dot{V}_1 = e_1 \dot{e}_1 = e_1 (e_2 - c_1 e_1 + \dot{i}_{ah} - \dot{i}_{ah}) = -c_1 e_1^2 + e_1 e_2. \quad (15)$$

If  $e_2 = 0$ , then  $\dot{V}_1 = -c_1 e_1^2 \leq 0$ . The next step design is then needed, and  $e_2$  is only an intermediate variable in the actual control law.

Step 2. Sliding variable structure mode control is a form of variable structure control. When the moving point is close to the switching surface ( $s_c = 0$ ), it can be attracted in a convergent manner. The surface is referred to as the

sliding mode area, which is composed of end points. The general sliding mode controller exhibits linear convergent characteristics, and the global fast terminal sliding mode controller does so in a fast nonlinear way. This approach ensures that the state tracking error reaches zero in a finite time. Therefore, the GFTSM controller has excellent dynamic performance.

The sliding mode surface is defined as (16)

$$s_c = e_2 + \alpha e_1 + \beta e_1^{p_2/p_1} = x_2 - \dot{i}_{ah} + c_1 e_1 + \alpha e_1 + \beta e_1^{p_2/p_1} \quad (16)$$

$$= \dot{e}_1 + (c_1 + \alpha) e_1 + \beta e_1^{p_2/p_1}.$$

A new Lyapunov function  $V_2$  is proposed

$$V_2 = V_1 + \frac{1}{2} s_c^2. \quad (17)$$

The sliding mode parameters  $\alpha$ ,  $\beta$  are positive real numbers.  $p_1$  and  $p_2$  ( $p_2 < p_1 < 2p_2$ ) are positive odd numbers.

$t_s$  is the time from the initial state  $e_1(0) \neq 0$  to the equilibrium state  $e_1(t_s) = 0$ .

$$t_s = \frac{p_1}{(c_1 + \alpha)(p_1 - p_2)} \ln \frac{\beta + (c_1 + \alpha)e_1(0)^{(p_1 - p_2)/p_1}}{\beta}. \quad (18)$$

System reaches its equilibrium state in a finite time by setting parameters  $\alpha$ ,  $\beta$ ,  $p_1$ ,  $p_2$ .

When  $s_c = 0$ , according to Eq. (16),

$$\dot{e}_1 = -(c_1 + \alpha)e_1 - \beta e_1^{p_2/p_1}. \quad (19)$$

When the system is far from the equilibrium point, the system can converge in an exponential series by the nonlinear exponential  $\beta e_1^{p_2/p_1}$ , but when the system approaches the equilibrium point, the linear component  $(c_1 + \alpha)e_1$  has a faster convergence speed than that of the non-linear component  $\beta e_1^{p_2/p_1}$ . The control ensures that the system converges to the equilibrium point quickly and accurately.

The derivative of  $V_2$  is

$$\begin{aligned} \dot{V}_2 &= \dot{V}_1 + s_c \dot{s}_c \\ &= -c_1 e_1^2 + e_1 e_2 + s_c [\dot{e}_2 + \alpha \dot{e}_1 + \frac{p_2}{p_1} \beta e_1^{p_2/p_1 - 1} \dot{e}_1] \end{aligned} \quad (20)$$

According to Eq. (13)(10), Eq. (20) becomes

$$\begin{aligned} \dot{V}_2 &= -c_1 e_1^2 + e_1 e_2 + s_c [f(x_1) + bu - \ddot{i}_{ah} + c_1 \dot{e}_1 + \alpha \dot{e}_1 + \\ &+ \frac{p_2}{p_1} \beta e_1^{p_2/p_1 - 1} \dot{e}_1]. \end{aligned} \quad (21)$$

To make  $\dot{V}_2 < 0$ , the global fast terminal mode controller is designed as

$$\begin{aligned} u &= \frac{1}{b} [-f(x_1) + \ddot{i}_{ah} - (\alpha + c_1) \dot{e}_1 - \frac{p_2}{p_1} \beta e_1^{p_2/p_1 - 1} \dot{e}_1 - \\ &- \frac{s_c}{|s_c|^2} (e_1 e_2) - c_2 s_c]. \end{aligned} \quad (22)$$

Substituting Eq. (22) into (21), the following equation is obtained:

$$\begin{aligned} \dot{V}_2 &= -c_1 e_1^2 + e_1 e_2 + s_c [-\frac{s_c}{|s_c|^2} (e_1 e_2) - c_2 s_c] = \\ &= -c_1 e_1^2 - c_2 s_c^2. \end{aligned} \quad (23)$$

When  $c_1, c_2 > 0$ ,  $\dot{V}_2$  is negative definite. If tracking error  $e_1 \neq 0$ , then  $V_2$  is positive definite. When  $|e_1| \rightarrow \infty$ ,  $|V_2| \rightarrow \infty$ . Therefore, the system is globally asymptotically stable. The error converges to zero in a finite time, according Eq. (18).

In Eq. (22), when  $e_1 = 0$  and  $e_1 \neq 0$ , the fourth term containing  $e_1^{p_2/p_1 - 1} \dot{e}_1$  may cause a singularity problem. However, this situation will not occur. According to Eq. (21), when the state reaches to the sliding surface,  $s_c$  is

close to zero, and  $\dot{e}_1$  is roughly equal to  $-(c_1 + \alpha)e_1 - \beta e_1^{p_2/p_1}$ .

Hence,  $e_1^{p_2/p_1 - 1} \dot{e}_1 = -(c_1 + \alpha)e_1 - \beta e_1^{p_2/p_1}$ . When  $p_1$  and  $p_2$  ( $p_2 < p_1 < 2p_2$ ) are positive odd numbers, both  $e_1^{p_2/p_1}$  and  $e_1^{2p_2/p_1 - 1}$  are non-singular. Therefore,  $e_1^{p_2/p_1 - 1} \dot{e}_1$  is non-singular.

## 4. SIMULATION STUDY

To verify the feasibility of the control algorithm, experiments are conducted using MATLAB /SIMULINK (R) with the Simpower toolbox. The simulation parameters are chosen as follows:

System parameters: the source voltage  $U_{s1} = U_{s2} = U_{s3} = 220V$ ,  $f = 50$  Hz. The nonlinear load resistance  $R_f = 10 \Omega$ , and the inductance  $L_f = 10$  Mh, the compensation circuit resistance  $R_C$  is  $0.1 \Omega$ , and the inductance  $L_C$  is  $10$  mH. Load parameters: nonlinear load begins to work from zero seconds, and then makes a stepwise change from  $0.12$  seconds. The proportional integral (PI) controller parameters: the capacitor voltage control in the dc-link is PI control,  $k_p = 0.05$ ,  $k_i = 0.01$ . The GFTSM controller parameters are as follows:  $c_1 = c_2 = 10000$ ;  $\alpha = 25000$ ;  $\beta = 50000$ ;  $p_1 = 5$ ;  $p_2 = 3$ .

Nonlinear loads include a three-phase rectifier bridges, resistance and inductance. After  $0.12$  s another three-phase rectifier bridge is fed into the simulation, forming a stepwise change of load to simulate the load changes.

### 4.1. PERFORMANCE ANALYSES OF HARMONIC SUPPRESSION IN THE APF

Figure 2 shows the transient current waveform of the load in phase A and the current waveform in phase A using the APF. As shown in Fig. 2, from  $0$  seconds to  $0.12$  seconds, the THD of the system is  $24.72\%$ . The APF is attached to the system from  $0.04$  s. The waveform of the system is improved. By applying FFT analysis to the waveform for two cycles from  $0.06$  s, the THD is reduced to  $1.61\%$ . In Fig. 3, the signal can track the harmonic changes in time after the APF starts to operate from  $0.04$  s. The APF can effectively filter out harmonics generated by nonlinear loads.

### 4.2. ANALYSIS OF FILTERING PERFORMANCE UNDER A CHANGING LOAD

By adding a nonlinear signal onto the load of phase A from  $0.12$  s, the load current exhibits a jump. From  $0.12$  s the system THD is  $22.24\%$  according to FFT analysis. The THD of the current waveform from  $0.12$  s to  $0.16$  s is  $5.19\%$ ; after  $0.16$  s it declines to  $1.52\%$ . Figures 4 and 5 show the results of signal FFT analysis from  $0.12$  s and from  $0.16$  s, respectively. The APF with GFTSM control based on backstepping design is found to be able to adapt to the load disturbance. After a transient time of approximately  $0.04$  s, the harmonic ratio decreases rapidly.

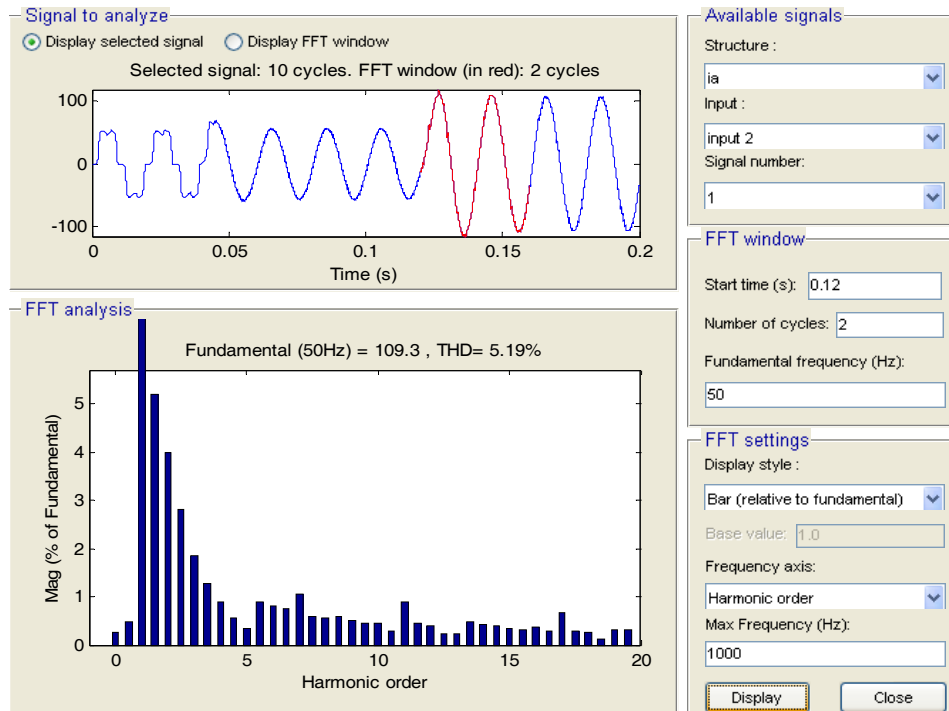


Fig. 4 – Current waveform and signal fft analysis from 0.12 seconds.

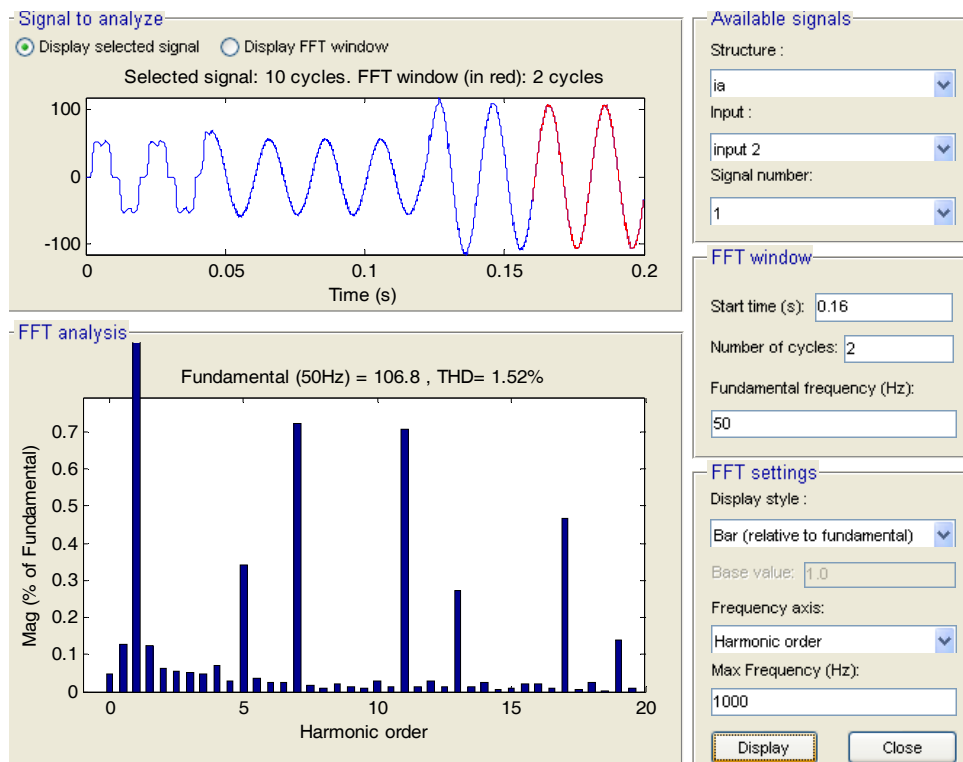


Fig. 5 – Current waveform and signal fft analysis from 0.16 seconds.

#### 4.3. FILTERING PERFORMANCE COMPARED WITH THE PURE BACKSTEPPING CONTROL

To verify the APF filtering performance using the proposed controller, a filter using pure backstepping controller is designed for the purpose of comparison. The parameters of backstepping controller are consistent with the GFTSM backstepping controller. The THD of the system is recorded from 0.12 s to the time when the system is basically stable.

The results are shown in Table 1, which compares the system THD between the pure backstepping controller and the GFTSM backstepping controller.

As shown in Table 1, after the same amount of time, the THD values of the system with the GFTSM backstepping controller is lower than those of the system with the pure backstepping controller, *i.e.*, the filtering effect with the GFTSM backstepping controller is better.

Table 1  
System THD of GFTSM backstepping control  
and pure backstepping control

Time(s)	THD(%)	
	GFTSM backstepping controller	pure backstepping controller
0.12	5.19	5.22
0.16	1.52	1.70
0.20	1.49	1.66
0.24	1.47	1.65
0.28	1.46	1.64

## 5. CONCLUSION

To effectively address the harmonics generated by non-linear loads in a three-phase three-wire system, a novel harmonic tracking algorithm for the APF was proposed in this paper. Comparing with the traditional backstepping controller, sliding mode control is added into backstepping control to improve the robustness of the APF. Furthermore, the GFTSM control makes the system reach the sliding surface in a finite time from any initial state, and improves the convergence speed of the control.

The results in Table 1 show that the filtering performance using the GFTSM backstepping control is better than single backstepping controller, and confirm the validity of the proposed GFTSM backstepping control applied to the APF system. In summary, the algorithm of APF controller has been designed and simulated in this paper. Moreover, the solution can have a chance to be supported experimentally, and in the next phase of work the focus will be more on the prototype design for application purpose.

## ACKNOWLEDGEMENTS

This work is partially supported by the National Science Foundation of China under Grant No. 61374100; the Natural Science Foundation of Jiangsu Province of China under Grant No. BK20131136; the Fundamental Research Funds for the Central Universities of China under Grant No. 2013B08914 and 2013B19314; and the Foundation of Jiangsu Key Laboratory Of Power Transmission and Distribution Equipment Technology in China under Grant No.2011JSSPD13.

Received on March 30, 2015

## REFERENCES

1. S. Chennai, *Three-Level Neutral Point Clamped Shunt Active Power Filter Performances Using Intelligent Controllers*, Rev. Roum. Sci. Techn. – Electrotechn. et Energ., pp. 303–313 (2014).
2. Y. Wan, J. Zhao, *Extended Backstepping Method for Single-Machine Infinite-Bus Power Systems With SMES*, IEEE Transactions on Control Systems Technology, pp. 915–923 (2013).
3. S. Shojaeian, J. Soltani, *Low Frequency Oscillations Damping of a Power System Including Unified Power Flow Controller Based on Adaptive Backstepping Control*, Rev. Roum. Sci. Techn. – Electrotechn. et Energ., pp.193–204 (2013).
4. A. Ghamri, M.T. Benchouia, A. Golea, *Sliding-mode Control Based Three-phase Shunt Active Power Filter, Simulation and Experimentation*, Electric Power Components and Systems, pp. 383–398 (2012).
5. J.T. Fei, S.X. Hou, *Adaptive fuzzy-sliding control with fuzzy-sliding switching for three-phase active power filter*, Transactions of the Institute of Measurement and Control, pp. 1094–1103 (2013).
6. Y. Feng, X.H. Yu, F.L. Han, *On nonsingular terminal sliding-mode control of nonlinear systems*, Automatica, pp.1715–1722 (2013).
7. H. Li, L.H. Dou, Z. Su, *Adaptive nonsingular fast terminal sliding mode control for electromechanical actuator*, International Journal of Systems Science, pp. 401–415 (2013).